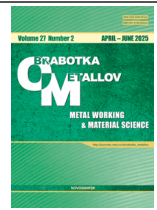## Obrabotka metallov –
Metal Working and Material Science

Journal homepage: http://journals.nstu.ru/obrabotka_metallov

Enhancement of EDM performance for NiTi, NiCu, and BeCu alloys using a multi-criteria approach based on utility function

Vijaykumar Jatti [1, a], Vijayan Singarajan [2, b], A. Saiyathibrahim [3, c], Vinaykumar Jatti [4, d], Murali Krishnan [2, e, *], Savita Jatti [5, f]

[1] School of Engineering and Applied Sciences, Bennett University, Noida, 201310, India

[2] Karpagam Institute of Technology, Coimbatore - 641105, Tamil Nadu, India

[3] University Centre for Research and Development, Chandigarh University, 140413, Punjab, India

[4] Symbiosis Institute of Technology, Symbiosis International (Deemed) University, Pune, 412115, Maharashtra, India

[5] D Y Patil College of Engineering, Savitribai Phule Pune University, Pune, India

[a] https://orcid.org/0000-0001-7949-2551, ✉ vijaykjatti@gmail.com; [b] https://orcid.org/0000-0002-3636-7731, ✉ s.n.vijayan@gmail.com;
[c] https://orcid.org/0000-0002-1968-0937, ✉ imsaiyath@gmail.com; [d] https://orcid.org/0000-0001-6016-0709, ✉ vinay.jatti89@gmail.com;
[e] https://orcid.org/0009-0004-0107-0753, ✉ murali15091990@gmail.com; [f] https://orcid.org/0000-0001-5514-8078, ✉ savitabirajdardyp@gmail.com

ARTICLE INFO

ABSTRACT

Introduction: Machining hard materials and shape memory alloys (*SMAs*), such as *NiTi*, *NiCu*, and *BeCu*, using conventional techniques is challenging due to excessive tool wear and poor surface finish. Non-conventional machining methods, particularly electrical discharge machining (*EDM*), offer improved precision and surface quality. However, the effectiveness of *EDM* is contingent upon the optimization of process parameters. The purpose of this study is to optimize *EDM* parameters to enhance the machining performance of *SMAs* by considering factors such as pulse-on time, pulse-off time, discharge current, gap voltage, and workpiece electrical conductivity. **Methods.** In this study, the *Taguchi* experimental design approach was employed to analyze the influence of key process parameters on the material removal rate (*MRR*), surface roughness (*SR*), and tool wear rate (*TWR*). Analysis of variance (*ANOVA*) was then applied to identify the most statistically significant factors affecting machining performance. A multi-objective optimization method, based on utility theory, was utilized to determine the optimal *EDM* settings that balance *MRR*, *SR*, and *TWR*. The results were validated through experimental trials. **Results and Discussion.** The experimental results indicated that Trial 15 achieved the highest *MRR* of 9.076 mm³/min, while Trial 1 produced the lowest *SR* of 2.238 μm. The minimum *TWR* of 0.041 mm³/min was observed in Trial 10, which contributes to increased tool lifespan. *ANOVA* revealed that gap voltage was the most influential factor, accounting for 85.98 % of the variation in machining performance, followed by discharge current (4.76 %) and pulse-off time (2.59 %). The multi-objective optimization process successfully identified parameter configurations that optimize *MRR* while minimizing *SR* and *TWR*. The prediction model developed in this study demonstrated high accuracy, with an R^2 value of 93.3% and an adjusted R^2 of 89.7%. Validation experiments confirmed the effectiveness of the optimized parameters, resulting in an average *MRR* of 8.852 mm³/min, *SR* of 2.818 μm, and *TWR* of 0.148 mm³/min. The findings presented herein confirm that careful optimization of *EDM* parameters significantly enhances the machining performance of *SMAs*, considerably improving machining efficiency and tool longevity.

* Corresponding author
Krishnan Murali R., D.Sc. (Engineering), Assistant Professor
Karpagam Institute of Technology,
Coimbatore – 641105, Tamil Nadu, India
Tel.: +91 9789339171, **e-mail:** murali15091990@gmail.com

Introduction

Advanced non-conventional electrical discharge machining (*EDM*) is an electro-thermal process where material is removed from a workpiece by means of electrical discharges (sparks). *EDM* is widely used in the manufacturing of shape memory alloy (*SMA*) components, ceramics, and composite materials due to its ability to provide high precision and geometric complexity [1]. *EDM* is considered one of the most effective methods for processing difficult-to-machine materials such as high-strength, brittle, and hard alloys, as it does not require the application of mechanical force [2].

During the *EDM* process, thermal energy required for material removal is generated by electrical sparks occurring in a dielectric fluid. Localized, intense heating caused by continuous electrical breakdowns leads to melting and vaporization of the workpiece material. The dielectric fluid performs several important functions: removing erosion products, cooling the workpiece, and preventing arc discharges [3].

Two types of *EDM* machines are distinguished: sinker *EDM* and wire *EDM* (*WEDM*). The selection of a specific type of *EDM* is determined by the application requirements, as well as the material properties and geometric parameters of the part being manufactured [4]. *EDM* enables the machining of electrically conductive materials with a wide range of mechanical properties. Due to its high precision and ability to meet specified surface quality requirements, *EDM* technology is in demand in the aerospace, automotive, biomedical industries, and in the manufacture of tools and dies [5].

EDM efficiency is determined by numerous process parameters, including discharge energy characteristics (pulse-on time and pulse-off time, current, gap voltage, spark gap), the type of electrode and dielectric fluid, flushing pressure, and cycle duration. Optimizing these parameters is a key factor in achieving maximum productivity (material removal rate), minimum surface roughness, and increased tool life [6].

Research in the field of *EDM* machining of advanced materials often includes parametric studies aimed at studying the influence of process parameters on material removal rate (*MRR, Q*), surface roughness (*SR, Ra*), and tool wear rate (*TWR, v_h*). These studies typically include an assessment of the underlying physical processes accompanied by parameter optimization methods. The results of such studies enable the development of *EDM* technologies suitable for high-performance applications requiring precise processing of difficult-to-machine materials [7].

Due to their improved mechanical and thermal properties, shape memory alloys (*NiTi*), Monel alloy (*NiCu*), and beryllium bronze (*BeCu*) are finding increasingly wide application, which increases the demand for *EDM* as an effective method for their processing. *NiTi* shape memory alloys exhibit both the shape memory effect and superelasticity, making them in demand in biomedical devices, the aerospace industry, and robotic systems [8]. Important properties of *NiTi* alloys include high corrosion resistance, biocompatibility, and the ability to elastically recover after deformation. *EDM* is the preferred method for processing such materials, as conventional machining methods are often ineffective due to the high strength and toughness of these alloys.

The *NiCu* material known as Monel alloy is characterized by excellent corrosion resistance combined with high mechanical strength and thermal stability. These properties make Monel alloy suitable for applications in marine environments, the chemical industry, and the aerospace sector. The difficulty in machining Monel alloy is related to the effect of strain hardening and high toughness, which makes *EDM* an optimal solution.

Beryllium bronze (*BeCu*) combines high strength, thermal conductivity, and corrosion resistance. The primary application areas of this alloy include electronic connectors, aerospace components, and tooling elements for injection casting. Hardening of beryllium bronze increases its strength, but the material becomes difficult to machine due to heat generation and tool wear [9].

To enhance the efficiency of the *EDM* process and reduce machining time, it is necessary to increase the material removal rate (*MRR, Q*). Surface roughness (*SR, Ra*) is an important quality indicator that determines the smoothness of the machined surface. *SR* is influenced by factors such as discharge energy, spark gap size, and dielectric fluid flushing conditions. When used in areas requiring precision machining, high surface quality requirements are imposed, which are achieved by minimizing *SR* values.

Tool wear rate (*TWR*, v_h) characterizes the rate of electrode material loss during the *EDM* process [10]. *TWR* depends on the gap current, electrode material, and dielectric fluid properties. Minimizing *TWR* is essential for reducing tool costs and increasing the economic efficiency of the process.

As a result of rapid solidification of the molten material removed by electrical discharge, a hardened layer known as the "*recast layer*" of a certain thickness is formed. Controlling the thickness of the recast layer is achieved by optimizing *EDM* parameters [11]. The area around the machined surface is subjected to thermal effects, forming a heat-affected zone (*HAZ*). Significant *HAZ* dimensions can lead to residual stresses and microcracks that affect the mechanical properties of the component. Managing the pulse energy and effectively using the dielectric fluid allows for improved thermal management. The microhardness of the machined surface may change due to thermal effects, which must be considered when evaluating the material characteristics after *EDM* [12].

Dimensional accuracy and overcut characterize the deviation of the machined part's dimensions from the specified values. The amount of overcut is influenced by the size of the spark gap, the pulse-on time, and tool wear. Achieving high dimensional accuracy is critical for the production of precision components. Adjusting the *EDM* process parameters allows for increased productivity, improved surface quality, and extended tool life in accordance with industry standards [13].

The *Taguchi* method is an effective statistical optimization technique widely used for various technological processes, including *EDM*. This method allows researchers to plan efficient experiments, optimizing process parameters with a minimal number of experimental runs. The main concept of the *Taguchi* method relies on orthogonal arrays (*OAs*) to simultaneously study the influence of several factors on the process output parameters [14]. The L18 *OA* is often used for *EDM* optimization, as it provides an effective assessment of the influence of various levels of process parameters. The *L18* array allows the analysis of up to eight factors, using two or three different levels of parameters, which is suitable for studying the main *EDM* parameters, such as pulse-on time, pulse-off time, current, and voltage [15].

Process optimization using the *Taguchi* method is based on the analysis of the signal-to-noise (*S/N*) ratio to determine the optimal values of parameters that provide the desired machining results. Three standard *S/N* ratio criteria are used in *EDM* studies: "*Smaller-the-better*" for minimizing *SR* and *TWR*, "*Larger-the-better*" for maximizing *MRR*, and "*Nominal-the-best*" for ensuring precision dimensional control. The *Taguchi* method can improve the efficiency of *EDM* by identifying optimal machining conditions by minimizing number of experiments and reducing cost and execution time while improving surface integrity and output productivity [16].

In the *EDM* process, several performance metrics must be considered simultaneously, as it requires achieving extreme *MRR* along with minimum *SR* and *TWR*. For balanced optimization of these competing criteria, the *Utility* method is often used, which is a popular tool for multi-criteria optimization. The *Utility* method transforms different output variables into a single combined index, simplifying the decision-making process. The application of the *Utility* method for *EDM* optimization involves the following steps: normalization of response values (bringing different performance characteristics to a comparable scale), assigning weights to each response based on its relative importance, and calculating a single utility value by multiplying the normalized values by the corresponding weights and summing the results. The optimal combination of process parameters is determined based on the maximum utility value, after which experimental verification is performed. The application of the *Utility* method allows manufacturers to find optimal parameter settings, providing an effective framework for balanced optimization of *EDM* performance indicators [17].

As a result of applying the *Utility* method, optimization of three key performance parameters of the *EDM* process was achieved, namely, *MRR*, *SR*, and *TWR*. The use of this method made it possible to balance the requirements for production speed and the quality of the machined surface. The integration of weighted normalization methods into the decision-making system improved its accuracy and reliability. The high process efficiency was made possible through the application of the *Taguchi* method, which provides a systematic study of the influence of *EDM* parameters with a minimal experimental test runs. The analysis of the *S/N* ratio allowed identifying critical parameters needed for accurate process optimization.

In addition, it was established that the electrical conductivity of the workpiece material, along with current and voltage measurements in the discharge, has a significant impact on machining performance and, in particular, on surface smoothness [18].

A detailed study of the machining methods of shape memory alloys (*SMAs*) was carried out, in which the effectiveness of *EDM* and its variations, including conventional die-sinking *EDM* and die-sinking micro-*EDM*, were evaluated. *SMAs*, possessing unique properties such as the shape memory effect, superelasticity, high corrosion resistance, and biocompatibility, particularly *NiTi*-based alloys and copper-based alloys, are widely in demand in various applications. *EDM* is a promising alternative to conventional machining methods, as it can solve problems related to tool wear, ensure high machining accuracy, and enables low-accuracy *CNC* machining. The present study focuses on analyzing the influence of *EDM* input parameters on response behavior when machining *SMAs*, with an emphasis on *NiTi* alloy systems.

The review examines various optimization strategies for *EDM* parameters, focusing on non-conventional approaches in addition to widely used statistical methods and multi-criteria decision-making methods. Particular attention is paid to both hybrid *EDM* methods and advanced technological approaches used in the processing of shape memory alloys [19].

An extensive review is devoted to the machining of shape memory alloys by *EDM*, with an emphasis on methods for processing *NiTi*-based *SMAs*. The wide industrial implementation of SMAs as industrial materials is emphasized due to their remarkable properties, finding applications in orthopedic implants, actuators, aerospace components, and biomedical devices.

It is noted that efficient machining of *NiTi SMAs* remains a complex challenge. This review analyzes experimental, theoretical as well as modeling and optimization-based approaches used to describe *EDM*, *WEDM*, and conventional machining processes for *SMAs*.

It is emphasized that improving machining efficiency requires optimal selection of process parameters, suitable electrode tools, and dielectric fluids. Among *EDM* methods, *WEDM* is the most extensively studied in the context of *SMA* cutting, outpacing die-sinking EDM and powder-mixed EDM used to enhance *SMA* processing performance and accuracy [20].

Several studies have investigated the optimization of *WEDM* process parameters for Nitinol shape memory alloys (nitinol – nickel-titanium alloy), which exhibit the ability to return to their original shape under the influence of thermal or mechanical factors. In [21], desirability function analysis (*DFA*) combined with the analytic hierarchy process (*AHP*) is used within a multi-criteria decision making (*MCDM*) framework to determine optimal machining conditions. The influence of four *WEDM* input parameters, namely, pulse-on time, pulse-off time, wire tension, and wire feed, on kerf width, *MRR*, and *SR* was investigated. Based on *DFA-AHP* methods, the optimal machining parameters were determined to be: pulse-on time 120 μs, pulse-off time 55 μs, wire tension 8 kgf, and wire feed 3 m/min. The results were confirmed by *S/N* ratio analysis using the *Taguchi* method. The combination of results showed that the *MCDM* approach successfully identifies effective process parameters to enhance the performance during the *WEDM* processing of Nitinol [21].

In [22], the *WEDM* of superelastic nickel-titanium *SMA* (*Ni54.1Ti*), driven by the difficulties of traditional machining methods investigated is studied. *NiTi*-based alloys require precision machining methods, especially in critical applications such as the medical industry. The assessment focused on the impact of pulse-on time, pulse-off time, and gap current on two key output metrics: *MRR* and *SR*. Experiments that systematically assessed these parameters were designed using a *Taguchi L27* mixed orthogonal array (*L27 OA*) and demonstrated that pulse-on time is a key parameter influencing the *MRR* and *SR* values [22]. The optimization of surface roughness of *NiTi SMA* in *EDM* using the *Taguchi* method was investigated in [23]. *NiTi*-based alloys are widely used as "smart" materials in various industries, including the security industry, the maritime sector, and the aerospace field, due to their unique properties. Due to the high hardness of this material, processing with conventional tools presents significant difficulties, making *EDM* a suitable solution. The machining quality of *NiTi* largely depends on surface roughness parameters. EDM process variables were optimized using a systematic *Taguchi* method to improve performance. The research results demonstrate the possibility of improving the surface quality of *NiTi*-based alloys and, therefore, confirm the effectiveness of *EDM* as a precision machining method for this challenging material [23].

Despite the difficulty in machining nickel-titanium (*NiTi*) *SMA* using conventional methods, *EDM* provides optimal performance when working with this material. However, high tool wear in *EDM* of *NiTi* leads to a reduction in the material removal rate. The study presented in [24] was aimed at maximizing *MRR* and minimizing *TWR* using the *Taguchi* method and the utility principle. Experiments were conducted on a die-sinking *EDM* machine in a liquid dielectric using a *Taguchi L36* mixed orthogonal array (22×33). *NiTi* alloy was used as the workpiece material, and copper was used as the electrode tool. *Taguchi* analysis revealed that workpiece and tool electrode electrical conductivity, gap current, and pulse-on time are the key factors influencing *MRR* and *TWR*. It was found that an *MRR* of 6.31 mm³/min and a *TWR* of 0.031 mm³/min are achieved with the following parameters: workpiece conductivity of 4219 S/m, tool conductivity of 26316 S/m, gap current of 16 A, and pulse-on time of 38 µs [24].

Reference [25] investigates the feasibility of processing nickel-titanium (*NiTi*) *SMAs* using *EDM* with copper, graphite, and tungsten-copper electrodes, and dielectric 358 as the dielectric fluid. The *EDM* process parameters included three levels of current (6, 12, and 18 A) combined with three values of pulse-on time (200, 400, and 600 µs) at a constant voltage of 3 V and a fixed pulse-off time of 50 µs. The primary objective was to determine the optimal settings to maximize *MRR* and minimize *SR* for *NiTi* shape memory alloys. The surface analysis of the workpiece included the examination of the electrode size and length using scanning electron microscopy (*SEM*) and energy-dispersive X-ray spectroscopy (*EDX*) to assess electrode material adhesion to the workpiece. Analysis of variance (*ANOVA*) was employed as a statistical method to determine the significance of process parameters. The differences between electrode materials were found to be relatively minor, and overcut was identified as the dominant factor influencing *MRR* and *SR*. Surface examination revealed the presence of surface defects in the form of droplets, debris, lumps, microcracks, and holes. Elevated *SR* values were associated with *Cu* and *W* residues from the electrode adhering to the workpiece due to insufficient dielectric rinsing [25].

Study [26] optimized the experimental conditions for surface milling of *NiTi SMA* under dry cutting conditions. The research aimed to achieve the lowest ***Ra*** and the minimal V_b using an uncoated tungsten carbide tool with a nose radius of 0.4 mm or 0.8 mm. Milling experiments were conducted at three cutting speeds (20, 35, and 50 m/min) and three feed rates (0.03, 0.07, and 0.14 mm/tooth) with a fixed axial depth of cut of 0.7 mm. A *Taguchi L18* orthogonal array was used as the design of experiment (*DOE*) method, utilizing *Minitab 17* software for data analysis. The analysis of variance (*ANOVA*) revealed that the cutting tool nose radius is the primary factor determining surface roughness, while the feed rate (f_z) has the greatest impact on flank wear (V_b). Confirmation tests verified that the optimal machining parameters accurately predict the results of the laboratory experiments, indicating the success of the optimization process [26].

The optimization of *EDM* parameters for *Cu*-based *SMA* components using machine learning (*ML*) algorithms is described in [27]. The optimization process focused on varying pulse-on time (T_{on}), pulse-off time (T_{off}), discharge current (I_p), and gap voltage (*GV*) to minimize tool wear rate (*TWR*). An empirical design of experiments (*DoE*) approach utilized a central composite design (*CCD*) in conjunction with response surface methodology (*RSM*) to analyze the machining behavior. The study employed both single- and multi-objective optimization using a desirability function approach, as well as genetic algorithms (*GA*) and teaching-learning-based optimization (*TLBO*) algorithms [27].

The optimization of process parameters significantly improved the efficiency of the corresponding machining methods. The innovative aspect of the presented research lies in the application of machine learning (*ML*)-based optimization techniques to the electrical discharge machining (*EDM*) of *Cu-SMAs*, opening new perspectives for the aerospace, biomedical, and automotive industries. Based on the results presented in [27], it can be concluded that precision machining benefits significantly from the implementation of "smart" materials and data-driven optimization methods.

A comprehensive analysis of existing shape memory alloys (*SMAs*) processing methods was conducted, encompassing both conventional and non-conventional approaches. The review includes research on waterjet machining (*WJM*), cryogenic machining, wire electrical discharge machining (*WEDM*), electrical discharge machining (*EDM*), and electrochemical machining. Key factors determining the performance and limitations of the considered processes are material removal rate (*MRR*), tool wear rate (*TWR*), surface

roughness (*SR*), and the integrity of the surface layer. Based on the analysis, the most effective *SMAs* machining methods were identified [28].

The optimization process of electrical discharge machining (*EDM*) for a high-temperature high-entropy shape memory alloy (*HT-HE-SMA*) with a composition of *35Ni-35Ti-15Zr-10Cu-5Sn* using a copper electrode is considered. It is emphasized that *EDM* is an effective method for machining complex-geometry parts from difficult-to-machine materials, and optimizing *EDM* process parameters can significantly improve the productivity and quality of the machined surface. The relationship between the input *EDM* process parameters — discharge current (I_p), pulse-on time (T_{on}), and pulse-off time (T_{off}) — and the output parameters, such as material removal rate (*MRR*), tool wear rate (*TWR*), and surface roughness (*SR*), was investigated. Response surface methodology (*RSM*) using a central composite design (*CCD*) was applied to evaluate the influence of machining parameters, and experimental data collection was performed using *Minitab 19* software. Based on analysis of variance (*ANOVA*) at a significance level of 5 %, the most significant factors were determined, and the adequacy of the second-order regression models was evaluated. It was found that discharge current, pulse-on time, and pulse-off time have a significant effect on *MRR*, *TWR*, and *Ra*. The high accuracy of the developed mathematical models was confirmed, as evidenced by the high coefficients of determination (R^2), reaching 97.82% for *MRR*, 99.53% for *SR*, and 95.36% for *TWR* [29].

The optimization of *EDM* parameters to achieve maximum *MRR* for *NiTi*, *NiCu*, and *BeCu* alloys was performed. Due to the difficulty of processing these advanced materials using conventional methods, *EDM* is considered an effective alternative. It is emphasized that the stability of the *EDM* process is a complex challenge due to the influence of numerous factors. This study investigates the optimization of *EDM* parameters by analyzing the current and voltage in the inter-electrode gap, combined with the control of pulse-on time, pulse-off time, and workpiece conductivity. A *Taguchi* orthogonal array was used for design of experiments (*DoE*), and *Taguchi*'s *S/N* ratio and *ANOVA* were used to determine the most significant factors affecting *MRR*. The results of the study demonstrate that *EDM* performance is largely dependent on the control of current and voltage in the gap, as well as pulse-on and pulse-off time [30].

The surface roughness (*SR*) and surface crack length (*SCL*) transformation in the *EDM* of electrolytic oxygen-free copper were evaluated using different processing modes. The influence of cryogenic treatment of the workpiece on *EDM* process parameters was investigated, including workpiece electrical conductivity, pulse-on time, pulse-off time, gap voltage, and gap current. The experiments were designed using a *Taguchi L18* orthogonal array and subjected to statistical analysis. The results showed that gap voltage, pulse-on time, and pulse-off time have the greatest influence on *SR*, while the interaction of workpiece conductivity with gap current, pulse-on time, and gap voltage affects the surface crack length. It was found that the surface cracks length initially decreases with increasing conductivity and then begins to increase. A decrease in gap current leads to an increase in crack length, while an increase in gap voltage promotes a decrease in crack length. Machine learning models applied for regression analysis demonstrated high accuracy in predicting *SCL* and *SR* parameters, achieving a coefficient of determination (R^2) exceeding 0.90 [31].

Tool wear rate (*TWR*) was minimized by optimizing the *EDM* parameters that influence the accuracy and cost-effectiveness of the process. Electrolytic copper was used as the electrode when machining *NiTi*, *NiCu*, and *BeCu* alloy workpieces. A *Taguchi L18* orthogonal array was used to analyze the influence of various factors on *TWR*. The factors considered were: workpiece conductivity, gap voltage and current, pulse-on time, and pulse-off time. *ANOVA* in combination with *Taguchi S/N* ratio analysis revealed that workpiece material conductivity, pulse-on time, and gap current have the greatest influence on *TWR*. Based on the results, a set of optimal parameters was determined, allowing for reduced tool wear and improved *EDM* productivity [32].

Another study investigated the effect of cryogenic treatment and an external magnetic field on the *EDM* of beryllium bronze (*BeCu*). Experiments were conducted using different values of gap current, magnetic field strength, and pulse-on time, as well as electrolytic copper electrodes. The highest *MRR* of 11.807 mm³/min was achieved when machining cryogenically treated *BeCu* workpieces with untreated copper electrodes. Among the parameters studied, only the gap current had a significant influence on *MRR*,

while the influence of pulse-on time and magnetic field strength was insignificant. Analysis of the surface microstructure using scanning electron microscopy (*SEM*) showed that a white layer with a thickness of up to 20 µm formed on the *BeCu* alloy after *EDM*, with minimal number of surface cracks [33].

Powder-mixed electrical discharge machining (*PMEDM*), as a promising machining method for difficult-to-cut alloys, particularly beryllium bronze (*BeCu*), is also being considered. The addition of fine powder particles to the dielectric fluid in *PMEDM* promotes increased machining efficiency and stability, as well as an increased concentration of spark discharges. A copper electrode was used in the experiments with constant pulse-on time, pulse-off time, and gap voltage. The gap current (ranging from 8–14 A) and powder concentration (2–6 g/L) were varied. The results showed that increasing the gap current and powder concentration leads to an increase in *MRR*. However, the worsening of flushing conditions at greater depths led to an increase in *TWR* [34].

In addition, the methods of manufacturing and processing beryllium bronze (*BeCu*)-based composite materials were investigated. The composite materials were fabricated using a stir casting, and their properties were evaluated using *SEM* and *EDX* methods. It was found that increasing the silicon carbide (*SiC*) particle content leads to an increase in material hardness. Abrasive waterjet machining (*AWJM*) was used to evaluate the machining performance of the composites, assessing *MRR* and hole circularity. The obtained parameters were compared with those obtained during *EDM*. *ANOVA* allowed for the identification of the most significant factors influencing the machining process, and the *Taguchi* method was used to optimize the parameters for achieving high productivity and accuracy [35].

The presented research stands out due to its novel approach to studying the peculiarities of the *EDM* process for three different materials: a shape memory alloy (*NiTi*), a monel alloy (*NiCu*), and beryllium copper alloy (*BeCu*). Special attention is paid to the difficulties encountered in processing these materials, due to their resistance to strength loss, thermal effects, and mechanical impacts. The results of the research can be valuable in industries such as aerospace, biomedical, and tool manufacturing.

The significance of the work is determined by the comprehensive approach, combining investigations of *EDM* characteristics for specific materials, multi-criteria optimization, and experimental verification, all of which are aimed at improving high-performance machining methods.

Materials and Methods

The primary purpose of this research was to identify optimal combinations of *EDM* parameters to achieve maximum productivity. The varied parameters included: workpiece material conductivity (S/m), gap current (A) and voltage (V), pulse-on time (µs), and pulse-off time (µs). The key output parameters characterizing process performance were material removal rate (*MRR*), surface roughness (*SR*), and tool wear rate (*TWR*). Therefore, the objective was to maximize the machining rate of difficult-to-machine materials through optimal selection of *EDM* parameters, followed by an evaluation of machinability.

NiTi and *NiCu* alloys (20 mm diameter, 20 mm length) and *BeCu* (20×20×30 mm³) were used as workpiece materials. Electrolytic copper was selected as the tool electrode material due to its high electrical conductivity. A copper rod (6 mm in diameter, 2000 mm in length) was cut and processed on a milling machine to obtain rectangular-shaped blanks, from which test samples (4×4×25 mm) were made. A square cave measuring 3×3 mm and 5 mm deep was formed in the samples using a tool electrode. The use of oxygen-free electrolytic copper ensured high electrical conductivity and wear resistance of the tool during the machining process.

The experiments were conducted on an *Electronica Machine Tool Limited* die-sinking *EDM* machine, model *C400x250*. Industrial *EDM* oil was used as the dielectric fluid. Side flushing at a pressure of 0.5 kg/cm² provided effective removal of erosion products and stability of the machining process. *GR-300* digital scales (accuracy 0.0001 g) were used to measure *MRR* and *TWR*, and a *Mitutoyo SJ 210* profilometer was used to measure surface roughness (*SR*). A more detailed description of the manufacturing process, experimental methods, and obtained results is presented in the previous work by *Vijaykumar S Jatt*i et al., 2022 [36].

A photograph of the die-sinking *EDM* machine used is shown in Fig. 1. The chemical, physical, and thermoelectric properties of the workpiece and tool materials are summarized in Tables 1 and 2, respectively. The research methodology is shown schematically in Fig. 2. Material removal rate (*MRR*) and tool wear rate (*TWR*) were calculated using equations (1) and (2):

$$MRR = \frac{\Delta W}{\rho_w t_m} \tag{1}$$

where ΔW is the change in workpiece mass (g); ρ_w is the workpiece material density (g/cm³); t_m is the machining time (min).

$$TWR = \frac{\Delta T}{\rho_t t_m} \tag{2}$$

where ΔT is the change in tool electrode mass (g); ρ_t is the tool electrode material density (g/cm³); t_m is the machining time (min).

Fig. 1. EDM die-sinking machine

<div align="right">T a b l e 1</div>

Chemical composition of materials used

Name of the material	*Ni* (%)	*Ti* (%)	*Be* (%)	*Cu* (%)
NiTi alloy	60	40	–	–
NiCu alloy	72	–	–	28
BeCu alloy	–	–	2	98
Copper electrode	–	–	–	99.9

The experimental design was developed and implemented using the *Taguchi* method. To enhance the statistical significance of the results, three repeated measurements were conducted for each parameter set, which is a requirement of the *Taguchi* method when using the signal-to-noise (*S/N*) ratio. The *S/N* ratio is a combined statistic that considers both the average value of the target characteristic and its variance distribution. Using this ratio allows for the optimization of process parameters to enhance overall performance.

Table 2

Physical properties of materials used

Name of the material	Density (ρ), g/cc	Specific heat capacity (c_p), J/gK	Melting point (H_m), K	Thermal conductivity (k), W/mk	Electrical conductivity (σ), S/mm
NiTi alloy	6.45	0.320	1583	10	3.268
NiCu alloy	8.8	0.427	1623	21.8	5.515
BeCu alloy	8.25	0.420	1253	130	5.645
Copper electrode	8.94	0.394	1356	391.1	10

Introduction

Problem identification and material selection

Selection of process parameters and response parameters

Selection of levels for the process parameters

Design of experiment using *Taguchi L18* orthogonal array

Execution of experiments with three replications

Measurement of response parameters

Calculation of signal-to-noise (s/n) ratios

Identify significant process parameters through analysis of variance (*ANOVA*)

Utilization of utility function to evaluate the overall desirability of machining performance

Determination of optimal process parameters based on the highest utility values

Prediction and validation through confidence intervals

Conclusions

Fig. 2. Methodology

Three main types of quality characteristics were used in the calculation of the *S/N* ratio: "Larger-is-Better" (*LB*) for *MRR* (aiming for the maximum response value), and "Smaller-is-Better" (*SB*) for *TWR* and *SR* (aiming for minimization). The "Nominal-is-Best" (*NB*) category is applied in cases where it is necessary to ensure precise adherence to a target value, for example, when maintaining specified dimensions. The mathematical expressions for calculating the *S/N* ratio corresponding to different quality characteristics are presented below (3), (4) and (5):

"Larger-is-Better"

$$(S / N)_{LB} - 10 \log \left(\frac{1}{R} \sum_{j=1}^{R} \frac{1}{y^2} \right) \tag{3}$$

"Smaller-is-Better"

$$(S / N)_{SB} - 10 \log \left(\frac{1}{R} \sum_{j=1}^{R} y^2 \right) \tag{4}$$

"Nominal-is-Best"

$$(S / N)_{NB} - 10 \log \left(\frac{1}{R} \sum_{j=1}^{R} (y_j - y_0)^2 \right) \tag{5}$$

where y_i is the the value of the parameter obtained in the i-th trial; R is the the number of repetitions of the trial; μ is the mean value of the data; σ is the standard deviation of the data.

In the *Taguchi* experimental design, an *L18* orthogonal array was used, selected based on the number of process parameters and their defined levels. The design included five parameters: workpiece electrical conductivity, gap current, gap voltage, pulse-on time, and pulse-off time. One variable (workpiece electrical conductivity) was varied at six levels, and the remaining four were varied at three levels. These parameters are designated as *A*, *B*, *C*, *D*, and *E*.

Table 3 presents the process parameters and corresponding levels used in the experiments. The *Taguchi* method requires the calculation of degrees of freedom (*DoF*) to select a suitable orthogonal array for design of experiments. The workpiece material electrical conductivity, having six measurement levels, determines five degrees of freedom. Each of the remaining four parameters (gap current, gap voltage, pulse-on time, and pulse-off time), varied at three levels, has two degrees of freedom per variable. Therefore, the total number of *DoF* is 13. Based on this, a mixed orthogonal array *L18* ($6^1 \times 3^4$) was chosen as satisfying the criterion of possessing seventeen degrees of freedom. The structure of the *L18* array is presented in Table 4.

The experiments were conducted in accordance with the *Taguchi L18* orthogonal array methodology. Two key principles of design of experiments (*DoE*) were implemented in this study. First, to enhance the statistical reliability of the results, the principle of replication was used, involving conducting multiple repeated measurements for each parameter set. This allows for improved accuracy in the estimation of main effects and their interactions, as well as a proper assessment of experimental error. In this study, three repeated measurements were conducted for each parameter combination. Second, data were collected for each experimental condition.

Based on the obtained data, the signal-to-noise (*S*/*N*) ratio was calculated for each experimental condition using equations (3)–(5), according to the selected quality characteristics (*MRR*, *TWR*, and *SR*). Analysis of variance (*ANOVA*) was used to determine the significance of the influence of various *EDM* process

Table 3

Process parameters and its levels

Parameters	Code	Levels					
		NiTi		*NiCu*		*BeCu*	
Electrical conductivity of workpiece (S/m)	*A*	3268 (untreated)	4219 (treated)	5515 (untreated)	5625 (treated)	5645 (untreated)	5902 (treated)
Gap current (A)	*B*	8	12	16	–	–	–
Gap voltage (V)	*C*	40	55	70	–	–	–
Pulse on time (μs)	*D*	13	26	38	–	–	–
Pulse off time (μs)	*E*	5	7	9	–	–	–

Table 4

Mixed *L18* ($6^1 \times 3^4$) orthogonal array

Trail No.	Parameter				
	A	*B*	*C*	*D*	*E*
1	1	1	1	1	1
2	1	2	2	2	2
3	1	3	3	3	3
4	2	1	1	2	2
5	2	2	2	3	3
6	2	3	3	1	1
7	3	1	2	1	3
8	3	2	3	2	1
9	3	3	1	3	2
10	4	1	3	3	2
11	4	2	1	1	3
12	4	3	2	2	1
13	5	1	2	3	1
14	5	2	3	1	2
15	5	3	1	2	3
16	6	1	3	2	3
17	6	2	1	3	1
18	6	3	2	1	2

parameters on the output characteristics. The significant and non-significant parameters of *EDM* process were identified by *ANOVA*. Statistical data processing was performed using *MINITAB 15.0* software.

The main effects plot visually displays the influence of each process parameter on the output characteristics, allowing for the assessment of trend changes. The response plot shows the change in the value of the output parameter as a function of the change in the level of the input parameter. The experimental program was executed three times for each parameter combination, after which data were collected. The analysis included both raw data analysis and *S/N* data analysis to determine the significance of the process parameters by comparing the main effects plots constructed based on *S/N* data and raw data.

Utility theory

Optimization based on utility theory allows for the quantitative assessment of product value, considering it as a combination of utility levels corresponding to different quality characteristics. The product optimization problem is reduced to maximizing overall utility by optimizing the individual utility of each characteristic.

The first step is to determine the optimal levels of the process parameters using the *Taguchi* method, which helps improve performance indicators. Then, a preference scale is established for each response (*MRR*, *SR*, *TWR*), taking into account the optimal and minimum values obtained during the experiments. The preference scale is constructed based on the following equation (6):

$$P_i = A \log \frac{x_i}{x'_i} \tag{6}$$

where P_i is the preference value for the i-th response; x_i is the raw data obtained from the experiment for the i-th response; x'_i is the smallest acceptable value for the i-th response; A is a constant, defined as:

$$A = \frac{9}{\log \frac{x'_i}{x_i}} \text{ (under optimal conditions)}$$

After determining the preference values for each response, it is necessary to determine the weightage (W_i, $i = 1, 2, ..., n$) for each performance indicator, satisfying the condition (7):

$$\sum_{i=1}^{n} W_i = 1. \tag{7}$$

Subsequently, for each test condition and repetition, the utility value ($U_{(n,R)}$) is calculated based on equation (8):

$$U_{(n,R)} = \sum_{i=1}^{n} P_i(n, R) x W_i \tag{8}$$

where n is the number of performance metrics (1, 2, 3, ..., 18); R is the number of repetitions of each trial (1, 2, 3).

After calculating the utility values, to determine the ideal configurations of process parameters, the S/N ratio is calculated, considering utility as a "Larger-the-Better" type of characteristic. Then, the average response value and confidence interval are calculated using the values of significant parameters. Equations (9) and (10) are used to calculate 95 % confidence intervals for confirmation experiments (CI_{CE}) and populations ($CIpop$):

$$CI_{CE} = \sqrt{F_{\alpha}(1, f_e)V_e \left(\frac{1}{n_{eff}} + \frac{1}{R} \right)} \tag{9}$$

$$CI_{pop} = \sqrt{\frac{F_{\alpha}(1, f_e)V_e}{n_{eff}}} \tag{10}$$

$F_{\alpha}(1, f_e)$ is the F ratio at the confidence level of (1-α) against DOF 1 and error degree of freedom f_e; V_e is the error variance; R is the sample size for confirmation trials.

$$N_{eff} = \frac{N}{1 + (DOF \text{ associated in the estimate of mean response})}$$

n_{eff} is an effective sample size, calculated as $N / (1 + DoF)$, where N is a total number of findings DoF is the total number of degrees of freedom associated with the estimation of the mean response.

Specific values:
N_{eff} = 54/(1+6) = 7.714;
N (total number of results) = 18×3 = 54;
R (sample size for confirmatory trials) = 3;
V_e (error variance) = 0.05087;
f_e (error degrees of freedom) = 11.

Conduct the validation trials at the optimum process parameter settings and compare the results with the projected mean response values. The assumed weightage of quality characteristics was 0.33 for each MRR, SR and TWR ($WMRR$, $WTWR$ and WSR), and the utility value was calculated using equation 14.

The utility values are calculated for all 18 experimental conditions and three repetitions. Since utility is a quality criterion that favors higher values, the utility values were analyzed based on the average utility at each parameter level as well as the S/N ratio.

Results and discussion

The trials were conducted using the *Taguchi* analysis approach. *ANOVA* was used to identify the key components of the process. The *MRR*, *SR* and *TWR* calculated during the experiment are shown in Table 5. This table displays the outcomes of an electrical discharge machining (*EDM*) experiment, whereby the *MRR*, *SR*, together with *TWR* were evaluated using the *Taguchi* design of experiments. The trials were performed under different machining settings, and the associated *S/N* ratios were determined. The *S/N* ratio was used as a performance metric to determine the optimal machining parameters, with higher values preferred for *MRR* ("larger-the-better") and lower values for *TWR* ("smaller-the-better").

Table 5

Trial results for *MRR*, *SR* and *TWR*

Trail No.	*MRR* (mm^3/min)			*S/N* ratio (dB)	*SR* (µm)			S/N ratio (dB)	*TWR* (mm^3/min)			*S/N* ratio (dB)
	Run 1	Run 2	Run 3		Run 1	Run 2	Run 3		Run 1	Run 2	Run 3	
1	2,096	2,078	2,088	6,3917	2,238	2,244	2,242	7,0101	0,072	0,068	0,073	22,9708
2	4,456	4,556	4,667	13,1740	2,998	3,018	3,010	9,5675	0,109	0,113	0,111	19,0926
3	7,109	7,118	7,112	17,0411	3,704	3,716	3,712	11,3890	0,151	0,148	0,146	16,5744
4	4,011	3,948	3,923	11,9542	2,756	2,764	2,762	8,8203	0,048	0,054	0,052	25,7818
5	6,502	6,498	6,495	16,2560	3,404	3,398	3,406	10,6364	0,088	0,081	0,084	21,4750
6	4,168	4,145	4,152	12,3714	2,806	2,799	2,802	8,9504	0,242	0,234	0,239	12,4555
7	2,803	2,688	2,781	8,8055	2,794	2,786	2,792	8,9142	0,101	0,094	0,098	20,2013
8	3,328	3,336	3,329	10,4515	2,988	2,979	2,984	9,4950	0,159	0,154	0,161	16,0254
9	8,995	8,989	9,027	19,0883	3,026	3,032	3,029	9,6260	0,198	0,204	0,201	13,9354
10	3,098	3,108	3,102	9,8347	3,318	3,307	3,311	10,4018	0,044	0,039	0,041	27,6633
11	5,981	5,972	5,982	15,5316	2,648	2,654	2,652	8,4693	0,179	0,172	0,175	15,1215
12	6,256	6,259	6,266	15,9319	2,826	2,818	2,822	9,0111	0,221	0,227	0,223	13,0074
13	3,411	3,398	3,405	10,6415	2,898	2,896	2,902	9,2440	0,045	0,048	0,041	26,9825
14	3,081	3,075	3,085	9,7719	2,886	2,892	2,888	9,2140	0,176	0,172	0,179	15,1051
15	9,076	9,069	9,081	19,1572	3,002	2,992	2,988	9,5251	0,214	0,209	0,212	13,4865
16	2,805	2,803	2,798	8,9493	3,308	3,298	3,302	10,3773	0,081	0,074	0,072	22,4106
17	6,707	6,698	6,704	16,5254	2,762	2,766	2,758	8,8245	0,122	0,116	0,124	18,3648
18	6,031	6,022	6,026	15,6011	2,752	2,748	2,754	8,7909	0,258	0,262	0,254	11,7669

EDM operations heavily depend on *MRR* as the essential performance metric to measure material removal rate during specific periods. Each *MRR* measurement set contains three readings (*MRR1*, *MRR2*, *MRR3*), allowing *S/N* ratio calculation via their average value. The tests performed in Trial 15 (9.076 mm³/min) and Trial 9 (8.995 mm³/min) achieved peak *MRR* values, as their respective *S/N* ratios reached 19.1572 dB and 19.0883 dB. The results indicate that these particular machining parameters deliver high efficiency in material removal. Trial 1, along with Trial 16, exhibited the lowest *MRR* rates (2.096 mm³/min and 2.805 mm³/min, respectively), accompanied by *S/N* ratios that reached 6.3917 dB and 8.9493 dB. The obtained values indicate reduced performance in material removal tasks. The various results of *MRR* across trials point toward particular machining variables that directly affect the amount of material removed.

From the experimental value of *SR*, it is evident that the finest surface finish (lowest roughness and highest *S/N* ratio) was obtained for Trial 1 (*S/N* ratio: −7.0101 dB), which produced the smoothest surface with roughness values of *SR1* = 2.238 µm, *SR2* = 2.244 µm, SR3 = 2.242 µm. This indicates that the optimized *EDM* parameters in this trial resulted in minimal surface defects and better surface integrity. The poorest surface finish (highest roughness and lowest *S/N* ratio) was obtained for Trial 3 (*S/N* ratio: −11.3890 dB), recorded the highest roughness values (*SR1* = 3.704 µm, SR2 = 3.716 µm, *SR3* = 3.712 µm), leading to a poor-quality surface. This may be due to high discharge energy, excessive tool wear, or increased thermal stress causing deep craters and microcracks. Surface roughness values range from 2.238

μm to 3.716 μm, showing significant variation in surface finish across different trials. The *S/N* ratio varies between −7.0101 dB and −11.3890 dB, confirming that process parameters significantly influence surface quality. Trials with closely matched *SR1*, *SR2*, and *SR3* values indicate high repeatability and process stability (Trial 11: *SR1* = 2.648 μm, *SR2* = 2.654 μm, *SR3* = 2.652 μm). The utility value for raw data was calculated using the equation and is mentioned in the table 5.

The machining life duration, together with operational expenses, depends heavily on *TWR*. *S/N* ratios for *TWR* were determined from three repetition readings (*TWR1*, *TWR2*, *TWR3*) in each trial. The tool wear recorded was 0.041 mm³/min in Trial 10, which also achieved the highest *S/N* ratio of 27.6633 dB, indicating reliable machining performance. Tool life conditions for Trial 6 were found unfavourable because it experienced the most wear (0.239 mm³/min) alongside the lowest *S/N* ratio (12.4555 dB). The wide variation of *TWR* measurements between trials demonstrates that tool wear mainly depends on process variables, which include pulse-on time and pulse-off time, alongside current settings.

Multi-objective Optimization of Performance Measures

Taguchi's approach identifies the optimal levels of input variables to maximize a single response. However, these input variable settings may lead to adverse outcomes for other responses. Consequently, there is a need to determine an ideal configuration of process variables that provides near-optimal quality attributes across multiple criteria. *Taguchi's* approach combined with the utility concept was employed to determine the optimal levels of process variables for multi-objective optimization.

Optimal configurations of process variables and ideal values for specific performance measures are shown in Table 6. Based on the *Taguchi* optimization, the best set of machining parameters for different responses was identified. The maximum *MRR* was obtained with Trial 15, which had the optimal parameters of $A_5B_3C_1D_2E_3$, and the predicted optimal value of *MRR* is 9.767 mm³/min. The highest *MRR* is achieved with a combination of high gap current and moderate pulse-on and pulse-off time, ensuring efficient material removal.

T a b l e 6

Optimal settings of process parameters and predicted optimal value of response

Responses	Trail No.	Optimal set of process Variables	Predicted optimal response value
Maximum *MRR*	15	$A_5B_3C_1D_2E_3$	9.767 mm³/min
Minimum *SR*	1	$A_1B_1C_1D_1E_1$	2.2119 μm
Minimum *TWR*	13	$A_5B_1C_2D_3E_1$	0.00404 mm³/min

The minimum *SR* was obtained with Trial 1, with the optimal parameters of $A_1B_1C_1D_1E_1$, and the predicted optimal surface roughness value is 2.2119 μm. The lowest roughness is obtained using the lowest gap current and the shortest pulse-on time, reducing surface damage and improving finish quality.

The optimum tool wear rate (*TWR*) of the *EDM* process is achieved at Trial 13, with the optimal parameters of $A_5B_1C_2D_3E_1$. The predicted optimal value for the *TWR* is 0.00404 mm³/min. The lowest tool wear is achieved by optimizing the discharge energy and duty cycle, ensuring minimal electrode erosion.

The preference scale is calculated by Equation (11) for *MRR* (P_{MRR}), Equation (12) for *SR* (P_{SR}), and Equation (13) for *TWR* (P_{TWR}). When calculating the preference scale, the predicted values of the optimal responses are as follows: 9.767 mm³/min for *MRR*, 2.2119 μm for *SR*, and 0.00404 mm³/min for *TWR*. The experimental findings indicate that the minimum and maximum *MRR* range from 2.078 mm³/min to 9.081 mm³/min, the *SR* ranges from 2.238 μm to 3.716 μm, and the *TWR* ranges from 0.039 mm³/min to 0.262 mm³/min.

$$P_{MRR} = 13.03 \times \log \frac{x_i}{2}; \qquad (11)$$

$$P_{SR} = -39.945 \times \log \frac{x_i}{3.716}; \tag{12}$$

$$P_{TWR} = -4.98 \times \log \frac{x_i}{0.262}; \tag{13}$$

$$U_{(n.R)} = P_{MRR}(n, R) + W_{MRR} + P_{TWR}(n, R) + W_{TWR} + P_{SR}(n.R) + W_{SR}, \tag{14}$$

where **n** is a trial number; **R** is a repetition number; повторение *WMRR*, *WTWR* и *WSR* are the assumed values of weighting coefficients.

Specific values:

n (trial number) = 1, 2, 3, ..., 18;

R (repetition number) = 1, 2, 3… .

The utility values are computed using Expression (14) for 18 experimental conditions and three repetitions of *MRR*, *SR*, and *TWR*, as shown in Table 7 for both raw data and *S/N* ratios. Given that utility is a quality characteristic favoring larger values, the *S/N* ratio is calculated using Expression 3. The data from Table 7 are presented as main effect plots for both *S/N* ratios and raw data.

Table 7

Utility data

Trail No.	Raw data (Utility Values)			S/N ratio (dB)
	R1	*R2*	*R3*	
1	3.913	3.922	3.885	11.8358
2	3.356	3.333	3.406	10.5391
3	2.787	2.786	2.800	8.9149
4	4.226	4.095	4.115	12.3486
5	3.489	3.557	3.517	10.9327
6	3.040	3.068	3.050	9.6936
7	2.945	2.934	2.956	9.3822
8	2.559	2.603	2.558	8.2086
9	4.192	4.158	4.182	12.4184
10	2.742	2.853	2.807	8.9407
11	4.264	4.276	4.271	12.6095
12	3.825	3.823	3.830	11.6546
13	3.681	3.631	3.736	11.3215
14	2.540	2.541	2.527	8.0836
15	4.199	4.234	4.234	12.5103
16	2.137	2.218	2.227	6.8203
17	4.511	4.536	4.506	13.0980
18	3.798	3.792	3.803	11.5906

From the utility data (Table 7), it is clearly stated that the highest *S/N* ratio is obtained for Trial 17 (13.0980 dB), which has the best performance with the highest utility values. This suggests an optimal combination of *EDM* parameters, leading to improved overall machining quality. Conversely, in the case of the lowest *S/N* ratio, Trial 16 (6.8203 dB) shows the poorest performance, indicating suboptimal process parameters that result in low utility values. The utility values range from 2.137 to 4.536, showing significant variation in machining performance across different trials. Higher *S/N* ratios correlate with higher utility values, confirming the robustness of the optimal parameter settings. Some trials exhibit closely matched *R1*,

R2, and *R3* values (Trial 11: 4.264, 4.276, 4.271), suggesting high repeatability due to consistent process parameters. Trials with higher deviations between *R1*, *R2*, and *R3* indicate process variability, which could be caused by inconsistent spark energy, wire tension, or thermal effects.

Impact of process variables for utility function with S/N data

The provided main effects plot for *S/N* ratios visualizes the influence of process parameters on the *S/N* ratio derived from the utility function in an *EDM* experiment (Fig. 3). For *WEC* (workpiece electrical conductivity), the obtained levels are 3268, 4219, 5515, 5625, 5645, and 5902. The plot shows fluctuations in *S/N* ratios across different wire electrode compositions. The peak *S/N* ratio is observed around level 4219, indicating better performance. Performance decreases at levels 5645 and 5902, suggesting suboptimal wire materials for efficient machining.
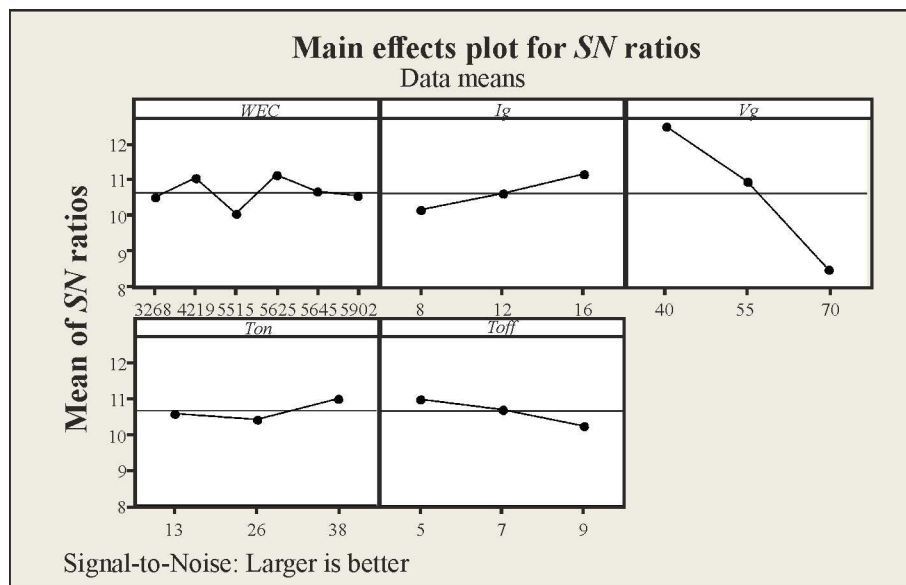

Fig. 3. Impact of process variables for utility function ($U_{MRR, SR, TWR}$) with *S/N* data

In the case of gap current (I_g), levels are 8, 12, and 16. The *S/N* ratio increases steadily with higher discharge current. Higher currents (e.g., level 16) improve performance, likely due to faster material removal. However, excessively high current could increase surface roughness and tool wear.

Considering gap voltage (V_g), the levels are 40, 55, and 70. The *S/N* ratio decreases significantly with increasing gap voltage. Lower voltages (e.g., 40) result in better *S/N* ratios, likely due to enhanced spark stability and controlled discharge energy.

T_{on} (pulse on time) was varied in the range from 13 µs to 38 µs (with an intermediate value of 26 µs). Analysis of the graph demonstrates a slight increase in the *S/N* ratio with increasing T_{on}. Longer pulse-on time ($T_{on} = 38$ µs) potentially improves the material removal rate while maintaining the required surface quality.

T_{off} (pulse off time) levels are 5, 7, and 9. The *S/N* ratio decreases with increasing T_{off}. Lower pulse-off times (e.g., 5) improve *S/N* ratios, likely due to reduced idle time and higher efficiency in spark discharge.

Gap voltage (V_g) has the most significant impact on the *S/N* ratio, as indicated by the steep slope of its main effects line. Gap current (I_g) and pulse on time (T_{on}) also show notable effects, although their trends are less steep compared to V_g. Pulse-off time (T_{off}) and *WEC* have comparatively less impact but still contribute to performance.

Optimal settings (based on larger *S/N* ratios) are given in Table 8.

Optimized *WEC*, gap current (I_g), and gap voltage (V_g) settings are critical for achieving a higher *S/N* ratio, reflecting better overall performance. Improper adjustments in V_g or T_{off} can significantly degrade performance, highlighting the importance of precise control in *EDM*.

Optimal setting parameter for S/N data

Sl.No	Parameter	Description
1	*WEC*	Level 4219 for optimal machining.
2	I_g	Level 16, as higher current improves material removal and reduces machining time.
3	V_g	Level 40, as lower gap voltage enhances spark stability.
4	T_{on}	Level 38, indicating that longer pulse-ON times are favorable.
5	T_{off}	Level 5, where shorter pulse-OFF times maximize machining efficiency.

Table 9 presents the pooled *ANOVA* results for the utility function that combines multiple performance measures (*MRR*, *TWR*, *SR*) derived from *S/N* data. The analysis evaluates the contribution and significance of process variables on overall performance. Below is a detailed breakdown.

ANOVA for utility function ($U_{MRR, SR, TWR}$) for SN data

Source	DoF	Seq SS	Adj SS	Adj MS	F-ratio	P-values	% contribution
I_g	2	3.141	3.141	1.5707	3.94	0.051	5.344
V_g	2	49.435	49.435	24.7174	61.96	0.000	84.102
T_{off}	2	1.816	1.816	0.9082	2.28	0.149	3.089
Residual error	11	4.388	4.388	0.3989	–	–	7.465
Total	17	58.780	–	–	–	–	100
$S = 0.6316$ R-Sq $= 92.5\%$ R-Sq(adj) $= 88.5\%$							

Each process variable (I_g, V_g, and T_{off}) has two degrees of freedom (*DoF*), corresponding to the levels tested for each parameter. The residual error has eleven degrees of freedom, representing variability unexplained by the factors. The total *DoF* is 17, which is the sum of all *DoF*.

The sequential sum of squares indicates the contribution of each factor to the total variability in the utility function. V_g (49.435) contributes the largest share of variability, indicating it has the most significant effect on performance. I_g (3.141) has a moderate impact, while T_{off} (1.816) has the least contribution among the three factors.

Adjusted sum of squares reflects the portion of variability accounted for by each factor after adjusting for other factors. The adjusted mean squares is obtained by dividing the adjusted sum of squares (Adj SS) by the degrees of freedom (*DoF*), representing the mean contribution of each factor to variability. The *F*-ratio is the ratio of adjusted mean square (Adj MS) to the mean square of residual error and determines the significance of each factor.

P-values test the null hypothesis that a factor has no effect. Significant factors include V_g ($P = 0.000$), which is highly significant (P < 0.05) and strongly influences the utility function. I_g ($P = 0.051$) is marginally significant, showing some influence on performance. T_{off} ($P = 0.149$) is not significant (P > 0.05), indicating minimal impact.

Gap voltage (V_g) dominates the utility function with an 84.102 % contribution, confirming its critical role in determining performance. I_g contributes moderately with 5.344 %, and T_{off} contributes minimally with 3.089 %. Residual error of 7.465% accounts for of unexplained variability.

S (0.6316) is the standard deviation of residuals, representing the goodness-of-fit; lower values indicate a better fit. R-Sq (92.5 %) is the proportion of total variability explained by the model, indicating that the

model explains most of the data variability. Adjusted R-Sq (88.5 %) accounts for the number of predictors in the model; it is slightly lower but still high, indicating a well-fitting model.

Gap voltage (V_g) is the most influential parameter, with an 84.102 % contribution to the utility function. Its P-value (0.000) indicates a statistically significant impact at the 95 % confidence level. Optimization of gap voltage is critical for improving *EDM* performance.

Discharge current (I_g) has a moderate influence, contributing 5.344 %. Its *P*-value (0.051) suggests it is marginally significant. Increasing gap current likely improves material removal but may also lead to trade-offs with surface quality.

T_{off} has minimal impact on the utility function, with only a 3.089 % contribution. Its *P*-value (0.149) indicates it is not statistically significant. Although the T_{off} adjustment is less critical, it can still affect processing efficiency and time.

The residual error accounts for 7.465 % of variability, which could be due to noise or unaccounted factors in the model. The model explains 92.5 % of the variability (R-Sq), with a strong Adjusted R-Sq of 88.5 %. This indicates that the utility function and process parameters are well represented by the model.

Since gap voltage has the highest contribution and significance, its optimization is critical for improving *EDM* performance. Gap current also impacts performance, though its effect is less dominant. Pulse-off time is less critical and may not require extensive optimization.

The utility function for *S/N* data yielded a response table with measurements from the utility of *MRR*, *SR*, and *TWR*. Table 10 demonstrates how the three process parameters – gap current (I_g), gap voltage (V_g), and pulse-off time (T_{off}) – influence the utility function that unites multiple responses ($U_{MRR, TWR, SR}$) through a single performance index.

Table 10

Response table with utility function ($U_{MRR, SR, TWR}$)
pertaining to *SN* data

Level	I_g	V_g	T_{off}
1	10.10	12.47	10.96
2	10.57	10.90	10.65
3	11.13	8.44	10.19
Delta	1.02	4.02	0.77
Rank	2	1	3

Each row shows the computed average utility function based on the specified factor levels. The utility performance at different gap current (I_g) levels demonstrates 10.108 at level 1, 10.570 at level 2, and reaches 11.130 at level 3. The difference between the maximum and minimum values (Delta) measures 1.022, reflecting the response variation due to I_g changes. The second rank position indicates that I_g affects the utility function with medium strength.

At V_g levels 1 through 3, the average utility values were measured as 12.470, 10.903, and 8.444, respectively. The maximum parameter difference (Delta) is 4.026, indicating that V_g is the strongest determining parameter, as confirmed by its first rank position — the highest in the analysis.

The utility function reveals T_{off} as the least influential factor during pulse-off time operations, with values at levels 1, 2, and 3 equal to 10.969, 10.653, and 10.195, respectively, and a Delta value of 0.774 – the lowest among all parameters. Its position at the bottom of the ranking confirms T_{off} as the least significant factor for the utility function.

Overall, the utility function shows that gap voltage (V_g) is the most important factor affecting the combined responses (*MRR*, *TWR*, *SR*). The evaluation with a Delta value of 4.026 validates V_g as the leading factor. The second most predominant factor is gap current (I_g), with a Delta value of 1.022. The response

is influenced by T_{off} but to a lesser extent than V_g. The effect of pulse-off time (T_{off}) remains minimal, with a Delta value of 0.774.

According to the ranking, V_g optimization should be the main priority for performance enhancement, followed by I_g management, while T_{off} modifications have minimal effect. Control of voltage stands as the critical parameter because it directly influences machining output, especially *MRR*, alongside *SR* and *TWR* performance. Voltage delivers the most significant impact on performance levels, followed by current. Changes in pulse-off time (T_{off}) have little impact on overall system operation because its duration plays a negligible role.

Impact of process variables for utility function with raw data

The main effects plot for means illustrates the influence of specific process factors on the mean utility values obtained from the experimental data. This plot helps determine the optimal levels of each parameter to enhance the effectiveness of the *EDM* process (Fig. 4).
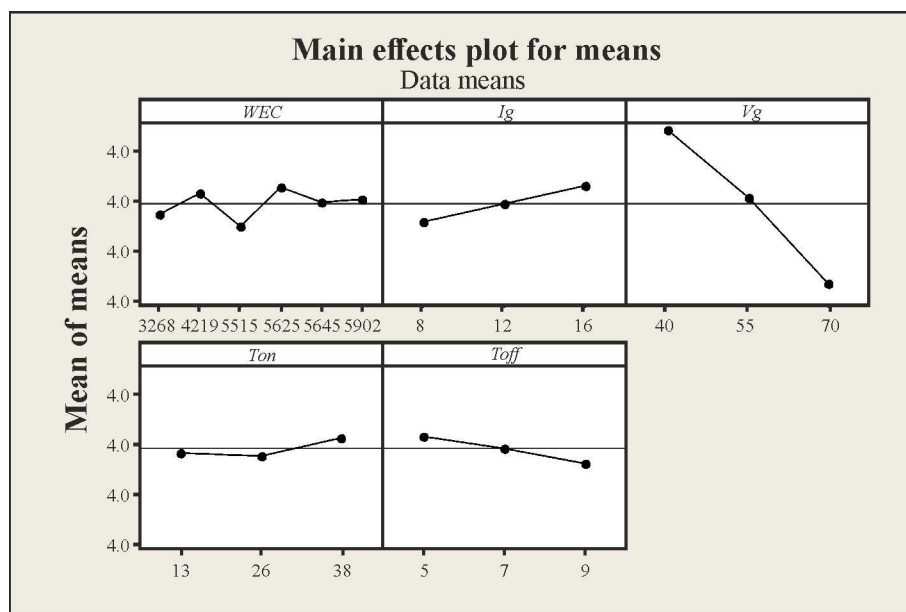

Fig. 4. Impact of process variables for utility function ($U_{MRR, SR, TWR}$) with raw data

Wire composition *ECW* (Levels: 3268, 4219, 5515, 5625, 5645, 5902):

The mean utility value fluctuates across different *ECW* levels. The highest mean is observed at level 4219, suggesting this wire composition is optimal for better performance. Conversely, the lowest mean at level 5515 indicates a suboptimal wire material for machining efficiency.

Gap current (I_g) (Levels: 8, 12, 16): the mean utility value increases steadily as the gap current increases. Higher current (16 A) results in better performance, likely due to faster material removal and enhanced efficiency. Lower current (8 A) leads to reduced performance, possibly because of insufficient spark energy for effective machining.

Gap voltage (V_g) (Levels: 40, 55, 70): the mean utility value decreases significantly with increasing gap voltage. The lowest voltage (40 V) produces the highest mean, likely due to improved spark stability and reduced arcing. Higher voltages (70 V) degrade performance, possibly owing to unstable discharge conditions and poor machining control.

Pulse-on time (T_{on}) (Levels: 13, 26, 38): the mean utility value slightly increases with longer pulse-on times. The highest level (38 μs) may improve material removal efficiency by enabling longer discharge duration. Lower levels (13 μs) result in marginally lower performance, potentially due to insufficient discharge duration.

Pulse-off time (T_{off}) (Levels: 5, 7, 9): the mean utility value decreases as pulse-off time increases. Shorter pulse-off time (5 µs) maximizes utility, likely due to reduced idle time and increased machining efficiency. Longer pulse-off times (9 µs) reduce performance, possibly because of decreased spark frequency.

ECW level 4219 is identified as the most suitable wire composition for achieving optimal performance. Gap voltage (V_g) has the most significant influence, with lower levels contributing to better utility values, underscoring the need for stable discharge conditions during machining. Gap current (I_g) and pulse-on time (T_{on}) must be optimized to achieve faster material removal and improved efficiency. Shorter pulse-off times (T_{off}) help maintain spark continuity, increasing machining effectiveness.

The optimal parameter settings for raw data are summarized in Table 11.

Table 11

Optimal setting parameter for raw data

Sl.No	Parameter	Description
1	WEC	Level 4219 (best wire composition)
2	Ig	Level 16 (higher discharge current)
3	Vg	Level 40 (lower gap voltage)
4	Ton	Level 38 (longer pulse-on time)
5	Toff	Level 5 (shorter pulse-off time)

Table 12 presents the pooled analysis of variance (*ANOVA*) for the utility function (**U**), which integrates multiple responses from the *EDM* experiments, including material removal rate (*MRR*), surface roughness (*SR*), and tool wear rate (*TWR*). The independent variables affecting the utility function are gap current (I_g), gap voltage (V_g), and pulse-off time (T_{off}). The table includes the following statistical terms:

– Degree of freedom (*DoF*) is the number of independent ways a factor can vary;
– Sequential sum of squares (*Seq SS*) is the total variation contributed by each factor;
– Adjusted sum of squares (*Adj SS*) is the sum of squares adjusted for other model terms or interactions;
– Adjusted mean square (*Adj MS*) is the variance of each factor, calculated as Adj SS divided by *DoF*;
– *F*-ratio is the ratio of factor variance to residual variance; higher values indicate stronger influence;
– *P*-value is the indicates statistical significance; values less than 0.05 denote significant effects;
– Percentage contribution is the proportion of total variation explained by each factor.

Table 12

ANOVA for utility function ($U_{MRR, SR, TWR}$) for raw data

Source	DoF	Seq SS	Adj SS	Adj MS	F-ratio	P-values	% contribution
I_g	2	0.4007	0.4007	0.20037	3.94	0.051	4.767
V_g	2	7.2282	7.2282	3.61411	71.05	0.000	85.984
T_{off}	2	0.2179	0.2179	0.10894	2.14	0.164	2.593
Residual error	11	0.5595	0.5595	0.05087	–	–	6.656
Total	17	8.4064	–	–	–	–	100
$S = 0.2255$ R-Sq = 93.3 % R-Sq(adj) = 89.7 %							

The gap voltage (V_g) has the highest impact, with an F-ratio of 71.05, the highest among all factors. The P-value is 0.000 (<0.05), confirming that it is statistically significant, with a contribution of 85.98 %. This indicates that V_g is the dominant factor affecting the utility function (U).

The gap current (I_g) has a moderate effect, with an F-ratio of 3.94, indicating some influence but lower than V_g. The P-value is 0.051, slightly above the significance threshold of 0.05, suggesting a marginally significant effect with a contribution of 4.76 %. This means that the impact of Ig is much lower than that of V_g.

The pulse-off time (T_{off}) has an insignificant effect, with an F-ratio of 2.14, indicating minimal influence. The P-value is 0.164, far above 0.05, confirming that it is statistically insignificant with a contribution of only 2.59 %, making it the least influential factor.

The residual error is 6.656 % of the total variation. This error term accounts for unknown or uncontrolled factors affecting the utility function. Since the error percentage is low (<10 %), the model is considered reliable.

The standard deviation (S) is 0.2255, which is a small value, indicating minimal variability and a good fit of the model. The R-Squared (R^2) value is 93.3 %, meaning that 93.3 % of the variation in the utility function is explained by the model. A substantial R^2 value indicates a strong relationship among input parameters and the response variable.

The adjusted R-squared (R^2 adj) is 89.7 %, which accounts for the number of predictors. Since it is close to R^2, this indicates that the model does not contain unnecessary terms, further confirming its reliability.

Table 13 demonstrates the effect of process parameters (I_g, V_g, and T_{on}) on the combined utility function, which integrates multiple responses (U_{MRR}, $_{SR}$, and $_{TWR}$) into a single index.

Table 13

Response table with Utility Function ($U_{MRR, SR, TWR}$)
pertaining to raw data

Level	I_g	V_g	T_{on}
1	3.27	4.20	3.59
2	3.46	3.52	3.47
3	3.64	2.65	3.32
Delta	0.36	1.54	0.26
Rank	2	1	3

The table displays the mean utility function values for each parametric level:

– for gap current (I_g), the utility function increases from 3.279 at level 1 to 3.464 at level 2, and further to 3.644 at level 3. The delta value is 0.365, indicating that changes in current have a moderate impact on the response outcomes. Although I_g significantly influences the utility function, it is not the primary determining factor.

– for gap voltage (V_g), the utility function values at levels 1, 2, and 3 are 4.207, 3.523, and 2.658, respectively. The highest delta value of 1.549 corresponds to V_g, making it the most influential parameter (Rank 1) affecting the utility function.

– for pulse-on time (T_{on}), the utility function values are 3.593 at level 1, 3.470 at level 2, and 3.324 at level 3. The delta value of 0.269 is the lowest among the parameters, indicating that T_{on} has the least impact on the utility function (Rank 3).

Gap voltage (V_g) is the primary influencing factor on the utility function due to its highest delta value (1.549). The variation of V_g creates substantial effects on the combined responses (U_{MRR}, $_{SR}$, and $_{TWR}$). The utility function shows a medium influence from the gap current parameter (I_g) according to its delta value

of 0.365. The least significant factor among these parameters is pulse-on time (T_{on}), based on its minimum delta value of 0.269. The best outcomes regarding *MRR*, together with surface roughness and tool wear, depend heavily on proper optimization of gap voltage (V_g). The selection process for gap current (I_g) needs optimization alongside gap voltage because it displays an important influence on performance. The variation of pulse-on time (T_{on}) leads to near-unnoticeable changes in the entire machining performance parameters.

Predicted optimal means

The optimal level of utility ($U_{MRR, SR, TWR}$) is anticipated at the ideal values of the main factors indicated above. The anticipated average of the performance metric may be calculated using equation (15):

$$\mu_{MRR,TWR,SR} = \bar{B}_3 + \bar{C}_1 + \bar{E}_1 - 2\bar{T} \tag{15}$$

where $\bar{T}$ is the overall mean of utility; $\bar{B}_3$ is the average value of utility at third level of gap current; $\bar{C}_1$ is the average value of utility at first level of gap voltage; $\bar{E}_1$ is the average value of utility at first level of pulse off time.

Specific values:

$\bar{T} = 3.462$;

$\bar{B}_3 = 3.644$;

$\bar{C}_1 = 4.207$;

$\bar{E}_1 = 3.593$;

$\mu_{MRR,TWR,SR} = 4.52$.

The 95 % confidence intervals for confirmation experiments (CI_{CE}) and the population (CI_{pop}) are computed using equations (9) and (10), with the results presented as follows:

$CI_{CE} = \pm 0.3376$ and $CI_{pop} = \pm 0.1787$

The estimated confidence interval for validation experiments is:

$$Mean_{\mu_{MRR,TWR,SR}} - CI_{CE} < \mu_{MRR,TWR,SR} < Mean_{\mu_{MRR,TWR,SR}} + CI_{CE}$$

$$4.1824 < \mu_{MRR,TWR,SR} < 4.8575$$

The 95 % confidence interval for the population is:

$$Mean_{\mu_{MRR,TWR,SR}} - CI_{pop} < \mu_{MRR,TWR,SR} < Mean_{\mu_{MRR,TWR,SR}} + CI_{pop}$$

$$4.3413 < \mu_{MRR,TWR,SR} < 4.6987$$

The confidence interval for confirmation experiments (CI_{CE}) defines the expected range of outcomes during the confirmation procedure. According to the experimental data, the true mean of the confirmation experiment results will lie between 4.1824 and 4.8576 with 95 % confidence. A broader interval width indicates higher variability and uncertainty in the experimental data.

The confidence interval for the population (CI_{pop}) predicts the natural variation present in the entire population across all possible observations. The narrower range of CI_{pop} indicates greater precision and less variability in the population data. Based on this confidence level, the measurement for the overall population should fall between 4.3413 and 4.6987.

The confidence interval for the confirmation experiments (CI_{CE}) is wider than that calculated for the population (CI_{pop}) because confirmation experiments rely on a smaller sample size, which increases measurement variability. Conversely, the larger dataset used to calculate CI_{pop} results in lower uncertainty.

Importantly, the true population mean (CI_{pop}) lies completely within the confirmation experiment range (CI_{CE}). A narrow population confidence interval combined with consistent experimental data is an excellent indicator that the data are both reliable and consistent with expected trends.

Precision increases as confidence interval widths decrease. The width of CI_{pop} directly correlates with the accuracy and certainty of the estimates. Confirmation experiment intervals tend to be wider than those of regular tests because they incorporate variability inherent in experimental results, while the narrower population interval offers better reliability in estimating the true mean due to its stability.

Wide confidence intervals indicate a high level of data variability, suggesting the need for improved optimization of experimental control parameters. The significant overlap between the two confidence intervals indicates that the experimental results statistically agree with the predicted values.

Confirmation experiments

The final step is to verify the achieved optimal levels of process variables by conducting experiments using these optimal values. The experiments were performed three times, and the average values were calculated. The average material removal rate (MRR) achieved was 8.852 mm³/min, the average surface roughness (SR) obtained was 2.818 μm, and the average tool wear rate (TWR) was 0.148 mm³/min.

The following expression (equation 16) was used to compute the utility value:

$$U = P_{MRR} \times W_{MRR} \times P_{SR} \times W_{SR} \times P_{TWR} \times W_{TWR};$$ (16)

$$U = 8.4434 \times 0.33 \times 4.7987 \times 0.33 \times 1.2352 \times 0.33 = 4.7775.$$

The empirically derived utility value 4.7775 lies within the 95 % confidence interval of the utility range estimated for the utility function ($U_{MRR, SR, TWR}$).

The determined MRR results from three experimental runs exhibit strong consistency, which confirms the stability of the selected process parameters (Table 14). The increased MRR measurement shows that the machining method succeeds at material removal while maintaining stable control of additional performance characteristics. MRR measurements between experimental runs show slight variations due to sparks energy variations and changes in material intrinsic properties. The measured surface roughness falls within a restricted range that represents outstanding process stability.

Table 14

Findings of confirmation experiments using optimal values of process variables

Response parameters	Optimal values of process variables	Obtained experimental value			Average value
		R1	*R2*	*R3*	
MRR (mm³/min)		8.825	8.898	8.832	8.852
SR (μm)	$A_2 B_3 C_1 D_3 E_1$	2.812	2.829	2.813	2.818
TWR (mm³/min)		0.143	0.154	0.147	0.148

The surface quality improves when the assessment value of SR decreases towards 2.8 μm, as this benefits precise components that need minimal manufacturing post-treatment. The selected parameters yield effective optimization of surface quality because run-to-run variations remain low. The production benefits from low TWR when electrode life extends and the cost of machining declines. The process stability is confirmed by the average TWR value of 0.148 mm³/min, as this indicates that the machining tools remain functional for extended period before electrode replacement is required. Small differences in TWR result from irregularities in electrical discharge power and workpiece material composition distribution.

Confirmation tests proved that the optimal manufacturing parameters generated from the multi-objective approach deliver expected results. The obtained experimental results matched well with the predicted values,

which proved the optimization method's reliability. The combination of high *MRR* and low *SR* and *TWR* shows that this *EDM* enables efficient high-quality machining suitable for use in automotive and aerospace components with demanding performance requirements.

Conclusions

The research offers a thorough assessment of the impact of process parameters on the utility function that combines *MRR*, *SR*, and *TWR* in *EDM*.

The experiments conducted in Trials 15 and 9 yielded *MRR* rates of 9.076 mm³/min and 8.995 mm³/min, together with *S/N* ratios measuring 19.1572 dB and 19.0883 dB, respectively. The machining parameters used in Trial 1 along with Trial 16 yielded the lowest *MRR* values of 2.096 mm³/min and 2.805 mm³/min, indicating insufficient material removal. The surface finish in Trial 1 achieved ideal effect due to its lowest roughness values (*SR1* = 2.238 μm, *SR2* = 2.244 μm, *SR3* = 2.242 μm) and the highest *S/N* ratio (−7.0101 dB). Trial 3 demonstrated poor surface quality with high roughness values (*SR1* = 3.704 μm, *SR2* = 3.716 μm, and *SR3* = 3.712 μm) due to excessive tool wear and the highest discharge energy, and also showed a low *S/N* ratio of −11.3890 dB. Trial 10 showed the best performance due to the minimum *TWR* of 0.041 mm³/min along with the best *S/N* ratio of 27.6633 dB.

The *Taguchi*-based optimization method has proven to be effective in finding the optimal machining conditions that provide the highest *MRR* performance along with the lowest *SR* and *TWR* results. *ANOVA* statistics confirm that pulse-on time, pulse-off time, and current play an important role in influencing the performance results during machining operations. The method shows the importance of precise control of *EDM* parameters to achieve the best machining results.

Each particular response (*MRR*, *SR*, and *TWR*) required individual optimal values for the machining parameters from the research findings. When dealing with multiple optimization objectives, utility theory helped develop a satisfactory compromise that provides uniform performance in each response area. The higher current level increases the material removal rate, but also results in a slight increase in surface roughness and tool wear. The main determinant of machining performance accounted for 84.102 % of the total utility function. The quality of the machining process performance improves when using lower voltage gaps, as this creates more reliable sparks. The surface quality remains high, as both material removal and pulse-on time increase together. The performance results are primarily determined by the pulse-off time, as this parameter contributes only 3.089 % to the overall score. The quality of the performance and the *S/N* ratio are best improved when the level is set to 4219.

The results show that the gap voltage (V_g) is the main influencing factor followed by the discharge current (I_g), while the pulse-off time (T_{off}) has no significant effect. A total of 92.5 % of the data variability (R^2) can be explained by the model, proving its high reliability in predicting the optimal machining scenarios. Trial number 17 achieved the optimal *S/N* ratio of 13.098 dB, which resulted in the best experimental results, thus becoming the optimal parameter setting among all the tested trials. In contrast, trial number 16 had the poorest experimental performance. The better machining quality exists as a direct consequence of the increased *S/N* ratios, demonstrating the success of the optimization strategy.

Optimizing the gap voltage is essential to achieving optimal *EDM* performance results. Increasing the discharge current accelerates material removal, but users need to manage it to prevent excessive tool degradation. The pulse-off time has little effect on operational efficiency, although shorter intervals improve performance. The utility approach applies various performance metrics to determine the optimal machining process that provides the highest efficiency and quality results. The gap voltage (V_g) process parameter showed the greatest impact on the utility function, as its delta values reached 4.026 for the *S/N* data, while reaching 1.549 for the raw data.

The *ANOVA* analysis yielded a *P*-value of 0.000, which was statistically significant, and the contribution rate to the results was 85.98 %. The impact of the gap current (I_g) on the utility function was moderate based on its delta values of 1.022 (*S/N* data) and 0.365 (raw data), resulting in a contribution of 4.76% according to *ANOVA*. The pulse-off time (T_{off}) was found to have the least impact on the utility function performance

as its delta values were the lowest at either 0.774 for S/N data or 0.269 for raw data. The *ANOVA* analysis confirmed that the contribution of the pulse-off time to the utility function performance was minimal (2.59 %), while its *P*-value (0.164) was high, proving statistically insignificant. The study found that *ECW* level 4219 in combination with I_g level 16, T_{on} level 38, V_g level 40 and T_{off} level 5 resulted in maximum *MRR*, *SR* and *TWR* results. Decreasing V_g and T_{off} values improved spark stability as well as machining efficiency, but increasing I_g and T_{on} rates resulted in improved material removal. High correlation existed between the input parameters and the utility function as shown by R^2 = 93.3 % and adjusted R^2 = 89.7 % in the statistical model. The model successfully predicts the response parameters as its residual error remains low at 6.656 %. Verification tests confirmed the most suitable process conditions resulting in an average *MRR* rate of 8.852 mm³/min along with *SR* values of 2.818 µm and *TWR* readings of 0.148 mm³/min. The experimental results fell within the specified 95 % confidence interval, confirming the robust and stable nature of the optimized processing parameters. The optimized process achieves excellent *MRR* levels along with minimal *SR* and *TWR*, making it suitable for precision manufacturing operations.

References

1. Sharma P., Kishore K., Sinha M.K., Singh V. Electrical discharge machining of nickel-based superalloys: a comprehensive review. *International Journal of Materials Engineering Innovation*, 2022, vol. 13 (3), pp. 157–190. DOI: 10.1504/IJMATEI.2022.125119.

2. Qudeiri J.E.A., Zaiout A., Mourad A.H.I., Abidi M.H., Elkaseer A. Principles and characteristics of different EDM processes in machining tool and die steels. *Applied Sciences*, 2020, vol. 10 (6), p. 2082. DOI: 10.3390/app10062082.

3. Philip J.T., Mathew J., Kuriachen B. Transition from EDM to PMEDM–impact of suspended particulates in the dielectric on Ti6Al4V and other distinct material surfaces: a review. *Journal of Manufacturing Processes*, 2021, vol. 64, pp. 1105–1142. DOI: 10.1016/j.jmapro.2021.01.056.

4. Slătineanu L., Dodun O., Coteaţă M., Nagîţ G., Băncescu I.B., Hriţuc A. Wire electrical discharge machining – a review. *Machines*, 2020, vol. 8 (4), p. 69. DOI: 10.3390/machines8040069.

5. Kamenskikh A.A., Muratov K.R., Shlykov E.S., Sidhu S.S., Mahajan A., Kuznetsova Y.S., Ablyaz T.R. Recent trends and developments in the electrical discharge machining industry: a review. *Journal of Manufacturing and Materials Processing*, 2023, vol. 7 (6), p. 204. DOI: 10.3390/jmmp7060204.

6. Gugulothu B., Aravindan N., Widjaja G., Lakshmanan S.A., Suresh M. Electrical discharge machining parameters and dielectric fluid: a review. *Handbook of Research on Advanced Functional Materials for Orthopedic Applications*, 2023, vol. 137–147. DOI: 10.4018/978-1-6684-7412-9.ch008.

7. Shastri R.K., Mohanty C.P., Dash S., Gopal K.M.P., Annamalai A.R., Jen C.P. Reviewing performance measures of the die-sinking electrical discharge machining process: challenges and future scopes. *Nanomaterials*, 2022, vol. 12 (3), p. 384. DOI: 10.3390/nano12030384.

8. Goyal A., Pandey A., Rahman H.U. Present and future prospective of shape memory alloys during machining by EDM/wire EDM process: a review. *Sādhanā*, 2022, vol. 47 (4), p. 217. DOI: 10.1007/s12046-022-01999-9.

9. Jatti V.S. Multi-characteristics optimization in EDM of NiTi alloy, NiCu alloy and BeCu alloy using Taguchi's approach and utility concept. *Alexandria Engineering Journal*, 2018, vol. 57 (4), pp. 2807–2817. DOI: 10.1016/j.aej.2017.11.004.

10. Bahgat M.M., Shash A.Y., Abd-Rabou M., El-Mahallawi I.S. Effects of process parameters on the machining process in die-sinking EDM of alloyed tool steel. *Engineering Design Applications III: Structures, Materials and Processes*. Springer, 2020, pp. 215–233. DOI: 10.1007/978-3-030-39062-4_19.

11. Harane P.P., Unune D.R., Ahmed R., Wojciechowski S. Multi-objective optimization for electric discharge drilling of waspaloy: a comparative analysis of NSGA-II, MOGA, MOGWO, and MOPSO. *Alexandria Engineering Journal*, 2024, vol. 99, pp. 1–16. DOI: 10.1016/j.aej.2024.04.049.

12. Liao Z., la Monaca A., Murray J., Speidel A., Ushmaev D., Clare A., Axinte D., M'Saoubi R. Surface integrity in metal machining – Part I: Fundamentals of surface characteristics and formation mechanisms. *International Journal of Machine Tools and Manufacture*, 2021, vol. 162, p. 103687. DOI: 10.1016/j.ijmachtools.2020.103687.

13. Ishfaq K., Farooq M.U., Pruncu C.I. Reducing the geometrical machining errors incurred during die repair and maintenance through electric discharge machining (EDM). *The International Journal of Advanced Manufacturing Technology*, 2021, vol. 117 (9), pp. 3153–3168. DOI: 10.1007/s00170-021-07846-1.

14. Hisam M.W., Dar A.A., Elrasheed M.O., Khan M.S., Gera R., Azad I. The versatility of the Taguchi method: Optimizing experiments across diverse disciplines. *Journal of Statistical Theory and Applications*, 2024, vol. 23 (4), pp. 365–389. DOI: 10.1007/s44199-024-00093-9.

15. Keskin G., Salunkhe S., Küçüktürk G., Pul M., Gürün H., Baydaroğlu V. Optimization of PMEDM process parameters for B$_4$C and B$_4$C+SiC reinforced AA7075 composites. *Journal of Engineering Research*, 2025, vol. 13 (1), pp. 47–56. DOI: 10.1016/j.jer.2023.09.012.

16. Zeng Y.P., Lin C.L., Dai H.M., Lin Y.C., Hung J.C. Multi-performance optimization in electrical discharge machining of Al$_2$O$_3$ ceramics using Taguchi base AHP weighted TOPSIS method. *Processes*, 2021, vol. 9 (9), p. 1647. DOI: 10.3390/pr9091647.

17. Sahoo S.K., Thirupathi N., Saraswathamma K. Experimental investigation and multi-objective optimization of die sink EDM process parameters on Inconel-625 alloy by using utility function approach. *Materials Today: Proceedings*, 2020, vol. 24, pp. 995–1005. DOI: 10.1016/j.matpr.2020.04.412.

18. Patel Gowdru Chandrashekarappa M., Kumar S., Pimenov D.Y., Giasin K. Experimental analysis and optimization of EDM parameters on HcHcr steel in context with different electrodes and dielectric fluids using hybrid Taguchi-based PCA-utility and CRITIC-utility approaches. *Metals*, 2021, vol. 11 (3), p. 419. DOI: 10.3390/met11030419.

19. Dutta S., Singh A.K., Paul B., Paswan M.K. Machining of shape-memory alloys using electrical discharge machining with an elaborate study of optimization approaches: a review. *Journal of the Brazilian Society of Mechanical Sciences and Engineering*, 2022, vol. 44 (11), p. 557. DOI: 10.1007/s40430-022-03826-y.

20. Singh R., Singh R.P., Trehan R. Machine learning algorithms based advanced optimization of EDM parameters: an experimental investigation into shape memory alloys. *Sensors International*, 2022, vol. 3, p. 100179. DOI: 10.1016/j.sintl.2022.100179.

21. Majumder H., Khan A., Naik D.K., Kumar C.S. Machinability assessment of shape memory alloy nitinol during WEDM operation: application potential of Taguchi based AHP–DFA technique. *Surface Review and Letters*, 2022, vol. 29 (01), p. 2250002. DOI: 10.1142/S0218625X22500020.

22. Gupta D.K., Dubey A.K. Multi process parameters optimization of Wire-EDM on shape memory alloy (Ni$_{54.1}$Ti) using Taguchi approach. *Materials Today: Proceedings*, 2021, vol. 44, pp. 1423–1427. DOI: 10.1016/j.matpr.2020.11.628.

23. Gangele A., Mishra A. Surface roughness optimization during machining of NiTi shape memory alloy by EDM through Taguchi's technique. *Materials Today: Proceedings*, 2020, vol. 29, pp. 343–347. DOI: 10.1016/j.matpr.2020.07.287.

24. Gaikwad V.S., Jatti V.S., Pawar P.J., Nandurkar K.N. Multi-objective optimization of electrical discharge machining process during machining of NiTi alloy using Taguchi and utility concept. *Techno-Societal 2018: Proceedings of the 2nd International Conference on Advanced Technologies for Societal Applications*. Springer International Publishing, 2020, vol. 2, pp. 479–489. DOI: 10.1007/978-3-030-16962-6_49.

25. Güven S., Yilmaz M., Gökkaya H., Nas E. Determination of the optimum conditions for machining NiTi shape memory alloys by electrical discharge machining. *Journal of the Institution of Engineers (India): Series C*, 2024, vol. 105 (5), pp. 1035–1046. DOI: 10.1007/s40032-024-01099-z.

26. Altas E., Gokkaya H., Karatas M.A., Ozkan D. Analysis of surface roughness and flank wear using the Taguchi method in milling of NiTi shape memory alloy with uncoated tools. *Coatings*, 2020, vol. 10 (12), p. 1259. DOI: 10.3390/coatings10121259.

27. Singh R., Singh R.P., Trehan R. State of the art in processing of shape memory alloys with electrical discharge machining: a review. *Proceedings of the Institution of Mechanical Engineers, Part B: Journal of Engineering Manufacture*, 2021, vol. 235 (3), pp. 333–366. DOI: 10.1177/0954405420958771.

28. Saoud F.B., Korkmaz M.E. A review on machinability of shape memory alloys through traditional and non-traditional machining processes: a review. *İmalat Teknolojileri ve Uygulamaları*, 2022, vol. 3 (1), pp. 14–32. DOI: 10.52795/mateca.1080941.

29. Al-Mousawi M.A., Al-Shafaie S.H., Khulief Z.T. Modeling and analysis of process parameters in EDM of Ni$_{35}$Ti$_{35}$Zr$_{15}$Cu$_{10}$Sn$_5$ high-temperature high entropy shape memory alloy by RSM approach. *Manufacturing Review*, 2024, vol. 11, p. 4. DOI: 10.1051/mfreview/2024002.

30. Gaikwad V., Jatti V.S. Optimization of material removal rate during electrical discharge machining of cryo-treated NiTi alloys using Taguchi's method. *Journal of King Saud University – Engineering Sciences*, 2018, vol. 30 (3), pp. 266–272. DOI: 10.1016/j.jksues.2016.04.003.

31. Sawant D.A., Jatti V.S., Mishra A., Sefene E.M., Jatti A.V. Surface roughness and surface crack length prediction using supervised machine learning-based approach of electrical discharge machining of deep cryogenically

treated NiTi, NiCu, and BeCu alloys. *The International Journal of Advanced Manufacturing Technology*, 2023, vol. 128 (11–12), pp. 5595–5612. DOI: 10.1007/s00170-023-12269-1.

32. Jatti V.S., Singh T.P. Optimization of tool wear rate during electrical discharge machining of advanced materials using Taguchi analysis. *WSEAS Transactions on Applied and Theoretical Mechanics*, 2016, vol. 11, pp. 44–53.

33. Sawant D., Bulakh R., Jatti V., Chinchanikar S., Mishra A., Sefene E.M. Issledovanie elektroerozionnoi obrabotki kriogenno obrabotannykh berillievo-mednykh splavov (BeCu) [Investigation on the electrical discharge machining of cryogenic treated beryllium copper (BeCu) alloys]. *Obrabotka metallov (tekhnologiya, oborudovanie, instrumenty) = Metal Working and Material Science*, 2024, vol. 26, no. 1, pp. 175–193. DOI: 10.17212/1994-6309-2024-26.1-175-193.

34. Bagane S., Jatti V.S., Singh T.P. Machinability study of beryllium copper by powder mixed electric discharge machining. *Applied Mechanics and Materials*, 2015, vol. 787, pp. 376–380. DOI: 10.4028/www.scientific.net/AMM.787.376.

35. Sankar V., Arravind R., Manikandan D. Material synthesis, characterization, and machining performance of stir cast beryllium copper alloy composites. *Transactions of the Canadian Society for Mechanical Engineering*, 2018, vol. 43 (2), pp. 143–152. DOI: 10.1139/tcsme-2018-0103.

36. Jatti V.S., Khedkar N.K., Jatti V.S., Dhall P. Investigating the effect of cryogenic treatment of workpieces and tools on electrical discharge machining performance. *AIMS Materials Science*, 2022, vol. 9 (6). DOI: 10.3934/matersci.2022051.

Conflicts of Interest

The authors declare no conflict of interest.